Adaptive Voltage Droop Method of Multiterminal VSC-HVDC Systems for DC Voltage Deviation and Power Sharing

Yizhen Wang, Weijie Wen, Chengshan Wang, *Senior Member, IEEE*, Haitao Liu, Xin Zhan, and Xiaolong Xiao

***Abstract*—Voltage source converter based multiterminal HVDC (VSC-MTDC) technology has shown many advantages. However, following a large disturbance, the dc voltage and the output power of the VSC station with fixed droop control may hit their limits, thereby reducing the dc voltage control ability of the whole MTDC system. Here an adaptive droop control scheme is proposed on the basis of both the dc voltage deviation factor and the power sharing factor. It contributes to ensure the dc voltage and the power loading rate of each converter within their limits during large disturbances, and the power sharing capability of the whole MTDC system remain high. The working principle of the proposed adaptive droop control is discussed in details. Case study and simulations are performed based on the PSCAD/EMTDC model of a ±320 kV four-terminal VSC-HVDC system to validate the effectiveness of the proposed adaptive droop method.**

***Index Terms*—VSC-MTDC, adaptive voltage droop method, power sharing, DC voltage deviation.**

I. Introduction

THE RAPID development of offshore wind farm projects far away from the coast, as well as the ring demand to connect the remote renewable energy sources to the major load centers, led to an increasing interest in high voltage direct current (HVDC) technology in the last decade. Compared with line-commutated converters, voltage source converters (VSCs) presents clear advantages due to the fully controlled semiconductors, such as gate turn-off thyristors and insulated gate bipolar transistors (IGBTs). VSCs enable better transmission efficiency, reactive power compensation, independent and flexible power control, and unlimited terminal configurations. With these advantages, VSC-HVDC provides a feasible choice for city centers in-feed, power supply to islands, grid connection, offshore wind energy integration, and multi-terminal HVDC (MTDC) systems [1]–[4]. Compared with the point-to-point HVDC system, MTDC systems have more advantages on enhanced reliability of the DC system, flexibility of power dispatch control, reduction in curtailment of renewable energy, and efficient utilization of converters and cables [5]–[7]. These distinguishing features make the VSC-MTDC system promising to transmit wind energy from offshore islands or to connect different grids in the future. Two VSC-MTDC demonstration projects have already been commissioned in China, namely, "Nan'ao ±160 kV three-terminal VSC-HVDC project" and "Zhoushan ±200 kV five-terminal VSC-HVDC project" [8], [9].

The VSC-MTDC system poses several challenges as the technology of different elements connected to the system is still evolving in terms of power and voltage levels. Given that DC voltage serves as an indicator of power balance and operation stability in an MTDC system, the DC voltage control of the VSC-MTDC system has become a priority to ensure overall system stability.

Theoretically, mainly three basic methods that control the DC voltage of the VSC-MTDC system, namely, (1) master-slave method, (2) the voltage margin method (VMM), (3) the voltage droop method (VDM), have been proposed. The first method can achieve high operation accuracy because the master converter can keep the DC voltage at the reference value and other slave converters can regulate power according to the power references [10], [11]. However, master-slave control method is tightly dependent on fast communication and the remote information is required. Since the DC voltage control is totally lost if the master converter fails, the master-slave control method suffers from poor reliability. To reduce dependency on fast communication and increase system reliability, decentralized control strategies such as VMM and VDM have been proposed. Reference [12] reviews VMM and different types of VDM methods. In VMM, one converter (master converter) is responsible for maintaining its DC voltage in the desired level, whereas other terminals operate at the constant power mode. Given some technical constrains, when the master converter is no longer able to supply or extract the active power necessary for controlling its DC voltage, another converter will operate as the master converter. However, a margin must be considered between the reference DC voltages of terminals. The transition between these two reference

Manuscript received January 27, 2018; revised April 3, 2018; accepted May 26, 2018. Date of publication June 6, 2018; date of current version January 22, 2019. This work was supported by the National Key Research and Development Program of China under Grant 2018YFB0904703. Paper no. TPWRD-00086-2018. *(Corresponding author: Weijie Wen.)*

Y. Wang, W. Wen, and C. Wang are with the Key Laboratory of Smart Grid of Ministry of Education, Tianjin University, Tianjin 300072, China (e-mail: yizhen.wang@tju.edu.cn; weijie.wen@tju.edu.cn; cswang@tju.edu.cn).

H. Liu is with the China Electric Power Research Institute, Beijing 100192, China (e-mail: lht@epri.sgcc.com.cn).

X. Zhan is with the State Grid Yangzhou Power Supply Company, Yangzhou 225000, China (e-mail: zhanxinstar@163.com).

X. Xiao is with the State Grid Jiangsu Electric Power Co., LTD, Nanjing 210000, China (e-mail: ethan518@126.com).

Color versions of one or more of the figures in this paper are available online at http://ieeexplore.ieee.org.

Digital Object Identifier 10.1109/TPWRD.2018.2844330

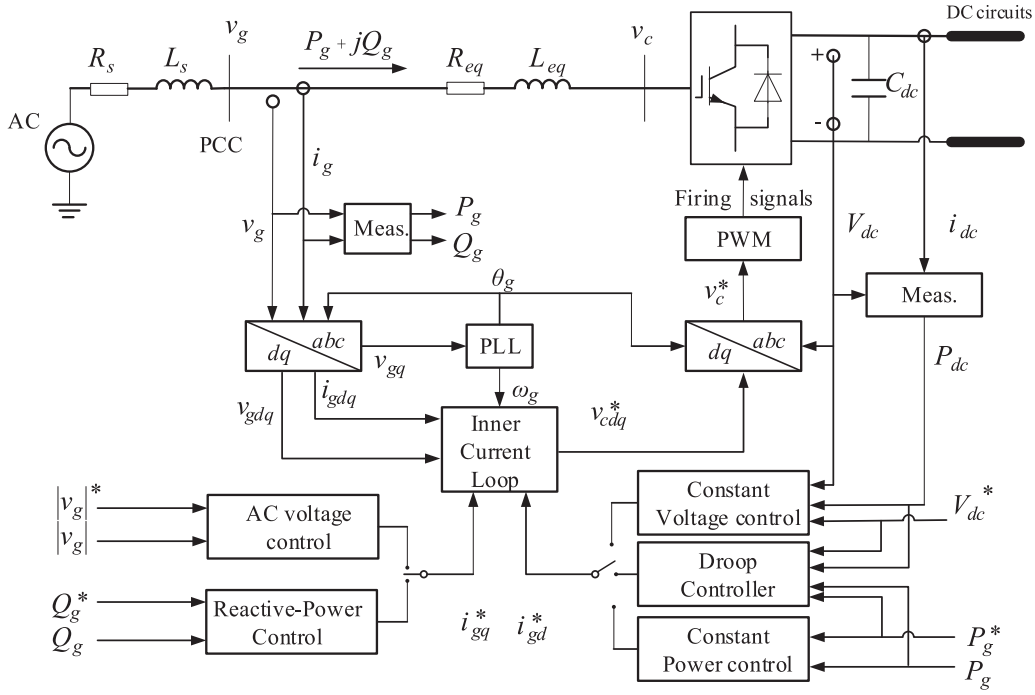

Fig. 1. The main diagram and control system of a VSC-HVDC station.

voltages places great stress on the converter. Moreover, the voltage margin must be large enough to avoid interactions between controllers [13], [14]. VDM is independent of communication. In VDM, which originates from power-frequency droop control in AC systems, all or some converters participate in regulating the DC voltage and sharing the power imbalance simultaneously in an appropriate way [15]. VDM exhibits higher reliability than the master-slave control and does not lead to voltage oscillation associated with VMM [12]. This feature is why VDM has attracted considerable research interest.

However, despite the popularity of VDM, problems caused by disturbance under fixed droop control cannot be neglected, including DC voltage deviating from its rated value [6], [16], [17], frequency deviation in the neighboring AC system [18], [19], and power flow calculation methods incorporating AC and DC systems [20]–[22]. One particular issue is how an MTDC system reacts to power disturbances such as loss/outage of one or more converters, DC line disconnection, and normal changes in power settings.

When a power disturbance occurs, the powers of the converters with fixed droop control may hit their limits; hence, such converters no longer contribute to power sharing, and the DC voltage deviation may be large. Reference [23] proposes a DC voltage droop design methodology that considers the different dynamics involving a VSC-MTDC system, but the calculation is complicated and the droop coefficients must be revised based on different operation conditions. Reference [24], [25] provide power-sharing control strategies that utilizes an adaptive VDM scheme based on optimal -power flow, but the computing time is slightly long. Reference [26] proposes a droop controller structure that maintains the DC voltage close to the nominal value and simultaneously attempts to preserve the power flow in the DC grid. Reference [27] introduces DC voltage regulation and frequency support in pilot voltage droop control by changing the reference operating point of voltage droop control, thereby maintaining adequate power sharing and efficient voltage regulation among the converter stations. However, the pilot voltage droop control needs a fast communication to transfer the measurements of DC voltages of different converter stations [28]. Reference [29] proposes a critical loading characterization method to identify the maximum exchange active powers for MTDC converters; this method is useful when connected to weak AC systems. Reference [30] introduces an efficient algorithm to adaptively determine the droop coefficients of MTDC converters to improve the stability margin of integrated AC/DC power networks. However, the transient performance of the whole system and the influence of DC voltage deviation are not considered. Reference [31] proposes a control scheme for adapting droop coefficients to share the burden in accordance with the available headroom of each converter station, but the DC voltage deviation of each converter is not considered during the transient process. Reference [32] points out that DC voltage deviation and power sharing capability are the two most important aspects of droop control, based on which a fuzzy logic based adaptive droop controller is proposed. However, only a basic fuzzy inference rule is formulated, which does not include a concrete equation or quantitative analysis.

On the basis of [31] and [32], this paper aims to propose an adaptive VDM scheme that ensures DC voltage deviations of the converters with droop control does not hit their limits during large events, and the power sharing capability of the whole

MTDC system remain high. The rest of this paper is organized as follows. In Section II, VSC structure and basic ideas of droop control are addressed. The adaptive VDM based on DC voltage deviation and power sharing is proposed in Section III. In Section IV, simulations of a four-terminal VSC-HVDC system under different disturbances have been done in PSCAD/EMTDC to validate the effectiveness of the proposed adaptive VDM. Finally, conclusions and future work are provided in Section V.

II. VSC Structure and Control Modes

A. Typical Structure and Control of a VSC-HVDC Station

The basic structure and control of a VSC-HVDC station is presented in Fig. 1 [26]. The adjacent AC system is equivalent to a Thevenin circuit of a fixed AC voltage source and serial impedance (R_s and L_s) at the point of common coupling (PCC). The converter transformer is not shown in this structure, but the inductances and resistances of the converter transformer and the bridges of VSC are modeled as an equivalent inductance L_{eq} with a small resistance R_{eq} in series. Modular multilevel converter (MMC) is one topology of VSC. The capacitors located at the DC terminals of the two-level VSC station or the paralleled DC capacitors of the sub-modules of MMC are symbolized as the capacitor C_{dc}. The VSC station is connected to other stations via DC circuits.

Typically, the control system of a VSC-HVDC station has two cascaded control loops, namely, the outer control loop and inner current control loop. The inner current control loop is implemented in the synchronously rotating *dq*-frame (voltage oriented), which makes the *dq*-frame current (i_{gd}, i_{gq}) track the current reference (i^*_{gd}, i^*_{gq}) rapidly by regulating the output voltage of the VSC. The current and the power in the VSC are directly governed by the inner current loop control in accordance with the reference generated by the outer loop.

The dynamics of the VSC station in Fig. 1 can be expressed in the rotating *dq*-frame as

$$\begin{cases} L_{eq}\dfrac{di_{gd}}{dt} = -R_{eq}i_{gd} + \omega_g L_{eq} i_{gq} - v_{cd} + v_{gd} \\ L_{eq}\dfrac{di_{gq}}{dt} = -R_{eq}i_{gq} - \omega_g L_{eq} i_{gd} - v_{cq} + v_{gq} \end{cases} \tag{1}$$

where (i_{gd}, i_{gq}), (v_{gd}, v_{gq}), and (v_{cd}, v_{cq}) denote the grid current, the voltage at PCC node, and output voltage of VSC in *dq*-frame, respectively. R_{eq}, L_{eq} denote the equivalent resistance and inductance between the PCC and VSC, respectively. ω_g is the electrical angular frequency.

The inner current control loop receives current references (i^*_{gd}, i^*_{gq}) and acts on the output voltage of the converter. The current in *dq*-frame can realize decouping control by adpting the voltage coupling compensations ($\omega_g L_{eq} i_{gd}$, $\omega_g L_{eq} i_{gq}$) and feedforward compensations of AC system voltage (v_{gd}, v_{gq}) in the inner current control loop. The detailed diagram of the inner current loop controller is shown in Fig. 2.

The outer controller is responsible for controlling the DC voltage and power of the VSC, which provides reference values to the inner current control loop. Depending on the DC voltage and power modes, which will be introduced in the following section, the reference values for the active current i^*_{gd} is provided by the constant voltage controller, constant power controller or droop controller, whereas the active current i^*_{gq} is provided by a reactive-power or AC voltage controller.

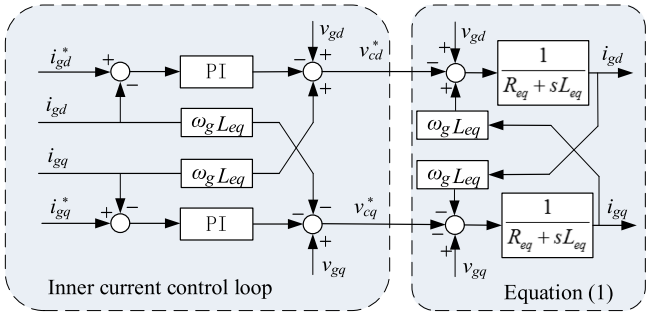

Fig. 2. The diagram of inner current loop controller.

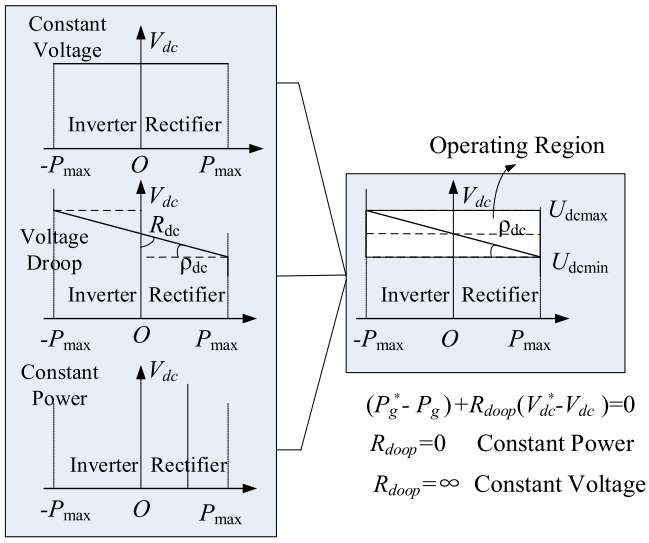

Fig. 3. The DC Voltage versus power characteristic curves of three control modes.

B. DC Voltage and Power Control Modes

A VSC-HVDC terminal may have one of three control modes, namely, constant power control mode, constant voltage control mode, and VDC mode. The DC voltage versus power characteristic curves of the three control modes are shown in Fig. 3. The constant voltage control mode maintains a constant DC voltage at the terminal regardless of the power flow change. The voltage V_{dc} will gradually become equal to the reference V^*_{dc}. The constant power control mode maintains a constant power flow of the converter regardless of the voltage level at that terminal. P_g will eventually be equal to the reference power P^*_g. The DC voltage control mode can be considered a combination of the two first types of VSC control modes. It attempts to control power to its reference level depending on the DC voltage deviation. Given that these two actions are somewhat contradicting, one action occurs at the cost of steady state deviation for the other. R_{droop} refers to the DC voltage response and is expressed by the unit MW/kV. The slope is given in terms of the DC droop coefficient ρ_{dc}, which is defined as the change in DC voltage per unit that

results in 100% change in converter power flow. R_{droop} is selected based on the maximum allowable DC voltage deviation to the rated value.

$$R_{droop} = \frac{P_{\text{rated}}}{V_{\text{rated}}\rho_{dc}} \tag{2}$$

where P_{rated} and V_{rated} refer to the rated power and rated DC voltage of the VSC, respectively.

At steady state, the relationship between DC voltage and the converter power is

$$(P_g^* - P_g) + R_{droop}(V_{dc}^* - V_{dc}) = 0 \tag{3}$$

Notable, the steady state characteristics in constant power control mode and constant DC voltage control mode are represented by DC voltage control controllers. In Fig. 3, if $R_{droop} = 0$, then droop control is regarded as constant power control; if $R_{droop} = \infty$, then droop control is regarded as constant DC voltage control. Thus, we can change the droop coefficient depending on the operating state of the VSC station to realize reasonable power sharing and voltage deviation.

III. Adaptive Droop Control for DC Voltage Deviation and Power Sharing

A. Fixed Droop

For an MTDC system with more than two converter stations, all the VSC stations with droop control should share the resulting power imbalance in a certain appropriate proportion following a large disturbance.

To simplify VDM, we assume that the MTDC system is an ideal lossless DC grid, and all DC bus voltages will be equal. These conditions imply

$$\Delta V_{dci} = \Delta V_{dc} \qquad i = 1, 2, ..., n \tag{4}$$

where ΔV_{dci} refers to the DC voltage deviation of the ith converter.

From (3), if the droop coefficient is fixed, then the power deviation ΔP_{gi} is expressed by

$$\Delta P_{gi} = -R_{droopi}\Delta V_{dci} \tag{5}$$

where ΔP_{gi} refers to the power deviation of the ith converter.

When a large imbalance power ΔP occurs in the MTDC system, the n VSC station with droop control will share the imbalance power by

$$\Delta P = \sum_{i=1}^{n} \Delta P_{gi} = \left(-\sum_{=1}^{n} R_{droopi} \right) \Delta V_{dc} = -R\Delta V_{dc} \tag{6}$$

where R is the DC voltage response of the DC grid (analogous to frequency response of AC grids), i.e., R shows the total amount of change in grid power flow in MW as a result of 1 kV change in DC bus voltage.

The imbalance power sharing of the ith converter is

$$\Delta P_{gi} = \frac{R_{droopi}}{\sum_{i=1}^{n} R_{droopi}} \Delta P = \frac{R_{droopi}}{R} \Delta P \tag{7}$$

From (7), the imbalance power sharing of the ith converter will exclusively be dependent on the DC voltage response R_{droopi} of the individual DC terminal and the total DC voltage response R of the MTDC system. When R_{droopi} rises, the imbalance power sharing will increase, and vice versa.

In general, the DC voltage response R_{droopi} of the ith VSC converter is designed in proportion to its capacity. However, powers and DC voltage deviations of converters with fixed droop control may reach their limits in case of unexpected events such as faults or disconnection of a station. This problem with fixed droop control can be avoided using an adaptive droop scheme described in the next subsection.

B. Adaptive Droop Control

For fixed droop control, the droop coefficients are usually dependent on the respective converter ratings. However, under a particular operating condition, all the converter stations with droop control may not be equally loaded and hit their limits. From (7), a relatively small R_{droop} (large ρ_{dc}) means the controller is restrictive toward power, allowing a small deviation of power in case of large deviation of V_{dc}. By contrast, a relatively large R_{droop} (small ρ_{dc}) indicates that the controller is restrictive toward voltage and will not allow a large deviation V_{dc} for a large deviation of power. The voltage deviation and power sharing are a trade-off.

The power headroom (difference between the rated capacity and present loading) is proposed to participate in power sharing [31]. However, the DC voltage deviation in transient and steady state is not considered. Reference [32] proposes a basic fuzzy inference rule: under the condition that the voltage deviation is large and power headroom is sufficient, the droop coefficient R_{droop} should be increased to ensure that the DC voltage is within a safe region. Otherwise, the droop coefficient should be reduced to ensure desirable power sharing. On the basis of the results proposed in [31] and [32], this paper proposes an adaptive droop control that consists of both the power sharing factor and DC voltage deviation factor.

$$R_{droopi}^{PV} = \alpha_i R_{droopi} \frac{H_{Pi}}{H_{Vi}} = \alpha_i R_{droopi} \frac{P_{\max i} - |P_{gi}|}{\xi - |\Delta V_{dci}|} \tag{8}$$

where R_{droopi}^{PV} refers to the adaptive DC voltage response coefficient. $H_{Pi} = P_{\max i} - |P_{gi}|$ refers to the power sharing factor of the ith converter. $H_{Vi} = \xi - |\Delta V_{dci}|$ refers to the DC voltage deviation factor. ξ refers to the limit of the DC voltage deviation, usually, $\xi = 5\%\ 10\%$. $\Delta V_{dci} = V_{dci} - 1$ refers to the DC voltage deviation from the rating voltage in per-unit. α_i is a user-defined positive constant, ensuring that the adaptive DC voltage response coefficient R_{droopi}^{PV} is equal to the given R_{droopi} in steady state. Thus, α_i is tuned by the operating state of the converter station (DC voltage and active power) and droop coefficient order (R_{droopi}) from the scheduling system or the energy management system.

As shown in Fig. 4, the DC voltage response coefficient will adaptively change based on the operating state of the converter station. This strategy ensures that the converters, which are already operating very close to the power limits, will not try to share the imbalance power, and the converters already operating very close to the DC voltage limits will not attempt to sacrifice

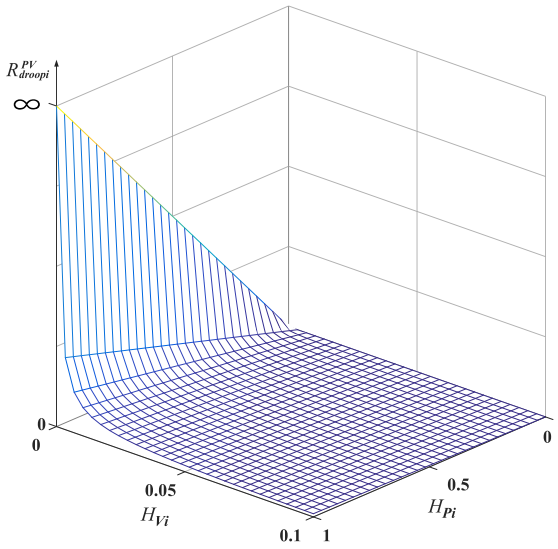

Fig. 4. The adaptive DC voltage response coefficient based on both the power sharing factor and the DC voltage deviation factor.

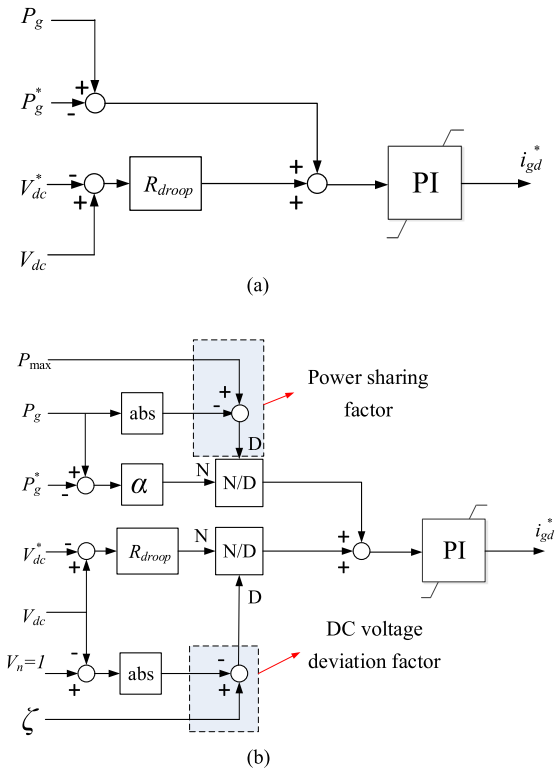

Fig. 5. The block diagram of voltage droop method. (a) The fixed droop control. (b) The proposed adaptive droop control.

DC voltage control ability for power sharing. The diagram of the proposed adaptive droop controller is shown in Fig. 5.

C. Discussion and Improvement

This section mainly discusses the control effect of the proposed adaptive droop scheme of a lossless MTDC system.

We assume that the loading ratio of VSC1 is the highest. VSC1 adopts the proposed adaptive droop control, whereas the other n–1 converters adopt fixed droop control. Once a large imbalance power ΔP occurs in the MTDC system, after substituting (8) into (7), the power sharing of VSC1 can be expressed by

$$\Delta P_{g1} = \frac{R^{PV}_{droop1}}{R^{PV}_{droop1} + \sum_{i=2}^{n} R_{droopi}} \Delta P \tag{9}$$

At the highest loading ratio of VSC1, the power sharing factor H_{Pi} adopts the predominant position than the DC voltage deviation factor H_{Vi}, resulting in the decrease in R^{PV}_{droop1}

From (9), the power sharing of VSC1 ΔP_{g1} decreases with R^{PV}_{droop1}, thereby ensuring that the power of VSC1 does not hit its limit. In particular, when there is no room for the power sharing, R^{PV}_{droop1} decreases to zero, and the control mode of VSC1 switches to constant power control.

Assuming all the VSCs with droop control modes adopt the proposed droop control, (7) can be rewritten as

$$\Delta P_{gi} = \frac{R^{PV}_{droopi}}{\sum_{i=1}^{n} R^{PV}_{droopi}} \Delta P = \frac{R^{PV}_{droopi}}{R^{PV}} \Delta P \tag{10}$$

In a lossless MTDC system, all DC bus voltages areequal, so the DC voltage deviation factors H_{Vi} are also equal. Thus, (10) can be transformed into

$$\Delta P_{gi} = \frac{\alpha_i H_{Pi} R_{droopi}}{\sum_{i=1}^{n} \alpha_i H_{Pi} R_{droopi}} \Delta P \tag{11}$$

From (11), in a lossless MTDC system, the power sharing of the converters with the proposed droop control scheme is not related to the DC voltage deviation factor H_{Vi}. The function of the DC voltage deviation factor H_{Vi} is to ensure that the DC voltage of the VSCs, which participate in voltage control, does not hit the voltage limits in transient and steady state.

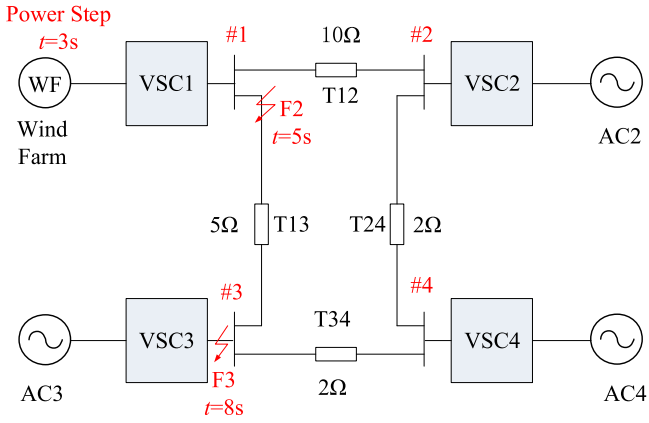

Fig. 6. The diagram of the four-terminal VSC-HVDC system.

IV. Simulation

This section adopts a four-terminal ±320 kV VSC-HVDC system under different disturbances in PSCAD/EMTDC to validate the effectiveness of the adaptive VDM discussed in Section III.

As shown in Fig. 6, the function of the MTDC system is to transfer power from a wind farm to three load centers. VSC1 is

TABLE I
THE PARAMETERS OF THE FOUR-TERMINAL VSC-HVDC SYSTEM

Symbol	Parameters	Value
v_l	line voltage of valve side ac system (rms)	370kV
L	The equivalent inductance of ac system	0.025H
R	The equivalent resistance of ac system	0.08Ω
C_0	Capacitance of each sub-module	1.4mF
N	Number of sub-modules of each bridge arm	200
L_s	Inductance of each arm bridge	0.25H
V_{dcn}	Rated dc-link voltage	±320kV
S_{n1}	Rated capacity of VSC1 station	2000MVA
S_{n2}	Rated capacity of VSC2 Station	400MVA
S_{n3}	Rated capacity of VSC3 Station	600MVA
S_{n4}	Rated capacity of VSC4 Station	1000MVA
f	Fundamental frequency	50Hz
f_s	Carrier frequency as multiple of fundamental	5
R_l	The unit resistance of the dc line	0.4Ω/km
L_l	The unit inductance of the dc line	0.45mH/km
l_{12}	The line length between VSC1 and VSC2	25km
l_{23}	The line length between VSC2 and VSC3	5km
l_{34}	The line length between VSC3 and VSC4	5km
l_{41}	The line length between VSC4 and VSC1	12.5km
ρ_{dc2}	The fixed droop coefficient of VSC2 in p.u.	0.025
ρ_{dc3}	The fixed droop coefficient of VSC3 in p.u.	0.0167
ρ_{dc4}	The fixed droop coefficient of VSC4 in p.u.	0.01
ζ	The limit of the DC voltage deviation in p.u.	0.05
K_d	Proportional gain of outer control loop	6
τ_d	Time constant of outer control loop	0.05
K_d	Proportional gain of inner control loop	0.6
τ_d	Time constant of inner control loop	0.01

a wind farm connected station, and it operates at the AC voltage control and constant frequency control mode (VF control mode). VSC2, VSC3 and VSC4 are the three AC grid-connected stations that operates at the VDM mode. The parameters of the four-terminal ±320 kV VSC-HVDC system are listed in Table I.

In this case, VSCs adopt MMC topology to avoid series of hundreds of IGBTs. Besides, carrier phase shift modulation method (CPSM) is adopted, and the carrier frequency is set to be 5 times fundamental frequency. The PI controller of the outer control loop in Fig. 5 is designed to achieve a closed loop bandwidth of 300 rad/s since the tracking parameters are DC in nature.

In the steady state, the output power of VSC1 station P1 is 1000 MW, VSC2, VSC3 and VSC4 station receives 110 MW, 258 MW and 580 MW, respectively. The DC voltages of VSC2, VSC3, and VSC4 station are 655.6 kV, 656.5 kV, and 654.3 kV, respectively.

The disturbances are set as follows:

1) $t = 3$ s, the output power of wind farm steps to 1400 MW.
2) $t = 5$ s, the DC line T13 between VSC1 and VSC3 station disconnects without faults (F2 in Fig. 6).
3) $t = 8$ s, VSC3 station disconnects from the MTDC system without faults (F3 in Fig. 6).

After adopting fixed droop control and the proposed adaptive droop control, the active power and DC voltage responses of the grid-connected VSC stations (VSC2, VSC3 and VSC4) under the above disturbances are shown in Figs. 7 and 8, respectively.

In the steady state before the first disturbance, the DC voltages and output power of the grid-connected VSC stations with the two control methods (fixed droop and proposed adaptive droop) are the same.

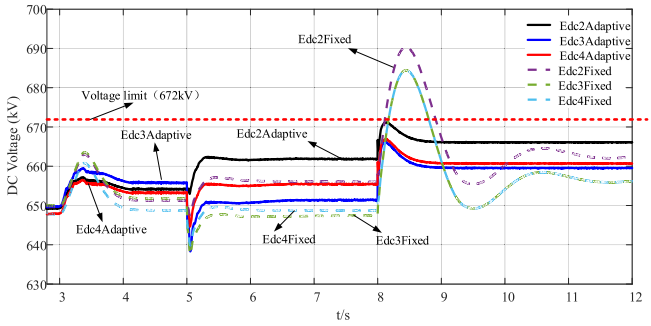

Fig. 7. The DC voltage simulation results of the grid-connected VSC stations under large disturbances. Where Edc2Adaptive, Edc3Adaptive and Edc4Adaptive denote the DC voltages of VSC2, VSC3 and VSC4 station with the proposed adaptive droop control scheme respectively. Edc2Fixed, Edc3Fixed and Edc4Fixed denote the DC voltages of VSC2, VSC3 and VSC4 station with fixed droop control scheme respectively.

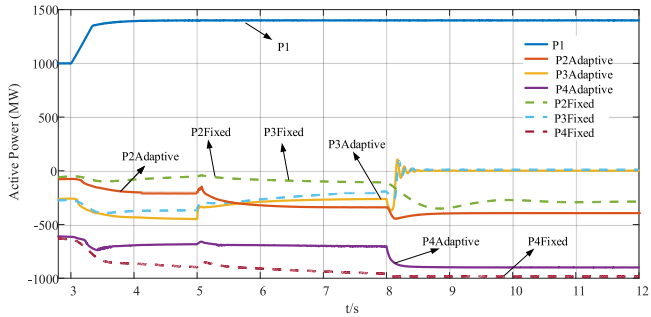

Fig. 8. The output active power simulation results of the grid-connected VSC stations under large disturbances. Where P2Adaptive, P3Adaptive and P4Adaptive denote the output active power of VSC2, VSC3 and VSC4 station with the proposed adaptive droop control scheme respectively. P2Fixed, P3Fixed and P4Fixed denote the output active power of VSC2, VSC3 and VSC4 station with fixed droop control scheme respectively.

When the output power of the wind farm steps to 1400 MW at $t = 3$ s, the DC voltages rise up to reduce the pressure of power sharing between the grid-connected VSC stations. Compared with fixed droop control, the DC voltages with the proposed adaptive droop control rise to a higher steady level more quickly, and the power loading rate of each grid-connected VSC is more balanced, thereby indicating the power sharing is more reasonable.

When the DC line T13 between VSC1 and VSC3 station disconnects at $t = 5$ s, the DC voltage and output active power reach a new steady state after some fluctuations. Compared with fixed droop control, the fluctuation is smaller and power sharing is more reasonable by adopting the proposed adaptive droop control scheme.

When VSC3 station disconnects from the MTDC system at $t = 8$ s, the output active power of VSC3 decreases to zero quickly, and the imbalanced power of VSC3 is shared by VSC2 and VSC4. Under the fixed droop control scheme, the output active power of VSC4 reaches its limit. Moreover, the fluctuation of DC voltage is large, thereby exceeding the DC voltage limit. Compared with fixed droop control, the proposed adaptive droop control ensures that the DC voltages of the grid-connected VSC stations (VSC2 and VSC4) are within their voltage limits, and

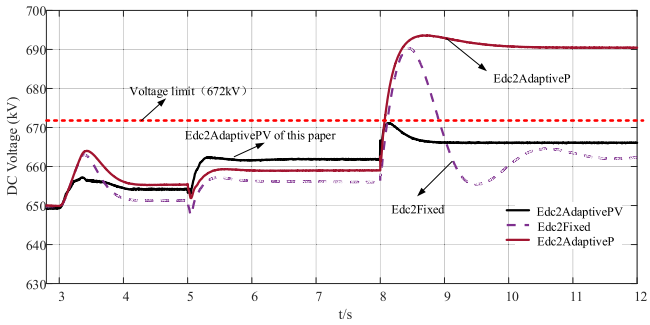

Fig. 9. The DC voltage simulation results of VSC2 with different droop control schemes under large disturbances. Where Edc2Fixed, Edc2AdaptivePV and Edc2AdaptiveP denote the DC voltages of VSC2 with fixed droop control scheme, adaptive droop control scheme of this paper and headroom-based power-sharing adaptive droop control scheme, respectively.

the power loading rates of the grid-connected VSC stations are almost equal and do not hit their power limits.

To validate the effectiveness of the proposed adaptive droop control further, the simulation of the four-terminal VSC-HVDC system with headroom-based power-sharing adaptive droop control is also conducted. A detailed comparison simulation results with the three droop methods (fixed droop control, the proposed adaptive droop control of this paper, and headroom-based power-sharing adaptive droop control) is shown in Fig. 9. The maximum DC voltage deviation of VSC2 with the proposed adaptive droop method is within the voltage limit, whereas those with fixed droop control and headroom-based power-sharing adaptive control exceeds the voltage limit. This result validates the effectiveness of the proposed adaptive droop control. Moreover, the response rate of the proposed adaptive droop control is fast, thereby shortening the transient process under large disturbances.

In sum, the simulations of the four-terminal VSC-HVDC system under large disturbances in PSCAD/EMTDC validate the effectiveness of the proposed adaptive droop control.

V. Conclusion and Future Work

The typical structure and control of a VSC station is introduced. The constant power control and the constant DC voltage control can be unified as special forms of VDM. Therefore, this paper proposes an adaptive VDM scheme for the grid-connected VSC stations.

Considering both the power sharing factor and the DC voltage deviation factor, an adaptive droop control is proposed to ensure DC voltage deviations within their limits during large disturbances, and the power sharing capability of the whole MTDC system remain high. A four-terminal VSC-HVDC system is established in PSCAD/EMTDC to validate the effectiveness of the proposed adaptive droop control.

Impacts of varying droop coefficients on the stability of the MTDC system, the adaptive droop control scheme considering frequency support, and impacts of line resistances on steady performance of the VSC-MTDC system with the proposed adaptive droop control [33] should be studied in the future.

References

[1] N. Flourentzou, V. G. Agelidis, and G. D. Demetriades, "VSC-Based HVDC power transmission systems: An overview," *IEEE Trans. Power Electron.*, vol. 24, no. 3, pp. 592–602, Mar. 2009.

[2] W. Lu and B.-T. Ooi, "Optimal acquisition and aggregation of offshore wind power by multiterminal voltage-source HVDC," *IEEE Trans. Power Del.*, vol. 18, no. 1, pp. 201–206, Jan. 2003.

[3] Y. Wang, Z. Yuan, and J. Fu, "A novel strategy on smooth connection of an offline MMC station into MTDC systems," *IEEE Trans. Power Del.*, vol. 31, no. 2, pp. 568–574, Apr. 2016.

[4] A. Lesnicar and R. Marquardt, "An innovative modular multilevel converter topology suitable for a wide power range," in *Proc. IEEE Power Tech. Conf.*, Bologna, Italy, 2003, vol. 3, pp. 1–6.

[5] M. K. Bucher, R. Wiget, G. Andersson, and C. M. Franck, "Multiterminal HVDC networks —What is the preferred topology?" *IEEE Trans. Power Del.*, vol. 29, no. 1, pp. 406–413, Feb. 2014.

[6] L. Xiao, Z. Xu, T. An, and Z. Bian, "Improved analytical model for the study of steady state performance of droop-controlled VSC-MTDC systems," *IEEE Trans. Power Syst.*, vol. 32, no. 3, pp. 2083–2093, May 2017.

[7] Y. Wang, Z. Yuan, J. Fu, Y. Li, and Y. Zhao, "A feasible coordination protection strategy for HB-MMC-MTDC systems under DC faults," *Int. J. Elect. Power Energy Syst.*, vol. 90, pp. 103–111, Sep. 2017.

[8] X. Li, Z. Yuan, J. Fu, Y. Wang, T. Liu, and Z. Zhu, "Nanao multi-terminal VSC-HVDC project for integrating large-scale wind generation," in *Proc. IEEE PES General Meeting*, National Harbor, MD, USA, 2014, pp. 1–5.

[9] C. Li, X. Hu, J. Guo, and J. Liang, "The DC grid reliability and cost evaluation with zhoushan five-terminal HVDC case study, " in *Proc. 50th Int. Univ. Power Eng. Conf.*, Stoke on Trent, U.K., 2015, pp. 1–6.

[10] L. Xu and L. Yao, "DC voltage control and power dispatch of a multiterminal HVDC system for integrating large offshore wind farms," *IET Renew. Power Gener.*, vol. 5, no. 3, pp. 223–233, May 2011.

[11] J. Zhu and C. Booth, "Future multi-terminal HVDC transmission systems using voltage source converters," in *Proc. Int. Univ. Power Eng. Conf.*, Cardiff, U.K., Sep. 2010, pp. 1–6.

[12] R. T. Pinto, S. F. Rodrigues, P. Bauer, and J. Pierik, "Comparison of direct voltage control methods of multi-terminal DC (MTDC) networks through modular dynamic models," in *Proc. 14th Eur. Conf. Power Electron. Appl.*, Aug./Sep. 2011, pp. 1–10.

[13] C. Dierckxsens, K. Srivastava, M. Reza, S. Cole, J. Beerten, and R. Belmans, "A distributed dc voltage control method for VSC MTDC systems," *Elect. Power Syst. Res.*, vol. 82, no. 1, pp. 54–58, 2012.

[14] R. T. Pinto, P. Bauer, S. F. Rodrigues, E. J. Wiggelinkhuizen, J. Pierik, and B. Ferreira, "A novel distributed direct-voltage control strategy for grid integration of offshore wind energy systems through MTDC network," *IEEE Trans. Ind. Electron.*, vol. 60, no. 6, pp. 2429–2441, Jun. 2013.

[15] K. Rouzbehi, A. Miranian, J. I. Candela, A. Luna, and P. Rodriguez, "A generalized voltage droop strategy for control of multiterminal DC grids," *IEEE Trans. Ind. Appl.*, vol. 51, no. 1, pp. 607–618, Jan./Feb. 2015.

[16] T. M. Haileselassie and K. Uhlen, "Impact of dc line voltage drops on power flow of MTDC using droop control," *IEEE Trans. Power Syst.*, vol. 27, no. 3, pp. 1441–1449, Aug. 2012.

[17] J. Beerten and R. Belmans, "Analysis of power sharing and voltage deviations in droop-controlled DC grids," *IEEE Trans. Power Syst.*, vol. 28, no. 4, pp. 4588–4597, Nov. 2013.

[18] N. R. Chaudhuri, R. Majumder, and B. Chaudhuri, "System frequency support through multi-terminal dc (MTDC) grids," *IEEE Trans. Power Syst.*, vol. 28, no. 1, pp. 347–356, Feb. 2013.

[19] W. Wang, Y. Li, Y. Cao, U. Hager, and C. Rehtanz, "Adaptive droop control of VSC-MTDC system for frequency support and power sharing," *IEEE Trans. Power Syst.*, vol. 33, no. 2, pp. 1264–1274, Mar. 2018.

[20] J. Lei, T. An, Z. Du, and Z. Yuan, "A general unified AC/DC power flow algorithm with MTDC," *IEEE Trans. Power Syst.*, vol. 32, no. 4, pp. 2837–2846, Jul. 2017.

[21] W. Wang and M. Barnes, "Power flow algorithms for multi-terminal VSC-HVDC with droop control," *IEEE Trans. Power Syst.*, vol. 29, no. 4, pp. 1721–1730, Jul. 2014.

[22] J. Beerten, S. Cole, and R. Belmans, "Generalized steady-state VSC MTDC model for sequential ac/dc power flow algorithms," *IEEE Trans. Power Syst.*, vol. 27, no. 2, pp. 821–829, May 2012.

[23] E. Prieto-Araujo, A. Egea-Alvarez, S. Fekriasl, and O. Gomis-Bellmunt, "DC voltage droop control design for multiterminal HVDC systems considering AC and DC grid dynamics," *IEEE Trans. Power Del.*, vol. 31, no. 2, pp. 575–585, Apr. 2016.

[24] M. A. Abdelwahed and E. F. El-Saadany, "Power sharing control strategy of multiterminal VSC-HVDC transmission systems utilizing adaptive voltage droop," *IEEE Trans. Sustain. Energy*, vol. 8, no. 2, pp. 605–615, Apr. 2017.
[25] R. Eriksson, J. Beerten, M. Ghandhari, and R. Belmans, "Optimizing DC voltage droop settings for AC/DC system interactions," *IEEE Trans. Power Del.*, vol. 29, no. 1, pp. 362–369, Feb. 2014.
[26] G. Stamatiou and M. Bongiorno, "Power-dependent droop-based control strategy for multi-terminal HVDC transmission grids," *IET Renew. Power Gener.*, vol. 11, no. 2, pp. 383–391, Jan. 2017.
[27] A. Kirakosyan, E. F. El-Saadany, M. S. E. Moursi, and K. A. Hosani, "DC voltage regulation and frequency support in pilot voltage droop controlled multi terminal HVDC systems," *IEEE Trans. Power Del.*, vol. 33, no. 3, pp. 1153–1164, Jun. 2017.
[28] A. Kirakosyan, E. F. El-Saadany, M. S. E. Moursi, S. Acharya, and K. A. Hosani, "Control approach for the multi-terminal HVDC system for the accurate power sharing," *IEEE Trans. Power Syst.*, vol. 33, no. 4, pp. 4323–4334, Jul. 2018.
[29] A. Moawwad, E. F. El-Saadany, M. S. E. Moursi, and K. A. Hosani, "Critical loading characterization for MTDC converters using trajectory sensitivity analysis," *IEEE Trans. Power Del.*, vol. 33, no. 4, pp. 1962–1972, Aug. 2018.
[30] A. Moawwad, E. El-Saadany, and M. S. E. Moursi, "Dynamic security-constrained automatic generation control (AGC) of integrated AC/DC power networks," *IEEE Trans. Power Syst.*, vol. 33, no. 4, pp. 3875–3885, Jul. 2018.
[31] N. R. Chaudhuri and B. Chaudhuri, "Adaptive droop control for effective power sharing in multi-terminal DC (MTDC) grids," *IEEE Trans. Power Syst.*, vol. 28, no. 1, pp. 21–29, Feb. 2013.
[32] X. Chen, L. Wang, H. Sun, and Y. Chen, "Fuzzy logic based adaptive droop control in multi-terminal HVDC for wind power integration," *IEEE Trans. Energy Convers.*, vol. 32, no. 3, pp. 1200–1208, Sep. 2017.
[33] L. Xiao, Z. Xu, T. An, and Z. Bian, "Improved analytical model for the study of steady state performance of droop-controlled VSC-MTDC systems," *IEEE Trans. Power Syst.*, vol. 32, no. 3, pp. 2083–2093, May 2017.

Yizhen Wang received the B.E.E. degree in electrical engineering from Tianjin University, Tianjin, China, in 2010, the M.E.E. degree in electrical engineering from China Electric Power Research Institute, Beijing, China, in 2013, and the Ph.D. degree in electrical engineering from Tsinghua University, Beijing, China, in 2017.

He is currently a Lecturer with the School of Electrical Engineering and Automation, Tianjin University. His current research interests include power system stability analysis, power system protection, and VSC-HVDC systems.

Weijie Wen was born in Shandong Province, China, in 1989. She received the B.E.E. degree in electrical engineering from Sichuan University, Chengdu, China, in 2012, and the Ph.D. degree in electrical engineering from Tsinghua University, Beijing, China in 2017. She is currently a Lecturer with the School of Electrical Engineering and Automation, Tianjin University, Tianjin, China. Her research interests include fast mechanical switch, current limiter, and direct current circuit breaker.

Chengshan Wang (SM'11) received the Ph.D. degree in electrical engineering from Tianjin University, Tianjin, China, in 1991. From 1994 to 1996, he was a Senior Academic Visitor with Cornell University, Ithaca, NY, USA. From 2001 to 2002, he was a Visiting Professor with Carnegie Mellon University, Pittsburgh, PA, USA. He is currently a Professor with the School of Electrical Engineering and Automation, Tianjin University, where he is also the Director of the Key Laboratory of Smart Grid of Ministry of Education. His current research interests include distribution system analysis and planning, distributed generation system and microgrid, and power system security analysis.

Haitao Liu was born in Shandong, China, in 1978. He received the B.S. degree in computer science and technology and the M.S. degree in electrical engineering from Beijing Information Science and Technology University and China Electric Power Research Institute in 2000 and 2008, respectively. He is currently an Electrical Professorate Senior Engineer with the China Electric Power Research Institute, Beijing, China. His research interests include smart grids and renewable energy generation systems.

Xin Zhan received the B.E.E. degree in electrical engineering from Hohai University, Nanjing, China, in 2010, and the Ph.D. degree in electrical engineering from Wuhan University, Wuhan, China, in 2015.

He is currently an electrical engineering staff with the State Grid Yangzhou Power Supply Company, Jiangsu Province, China. His current research interests include power system operation and control and distribution network dispatch.

Xiaolong Xiao is currently an Assistant Engineer with the State Grid Jiangsu Electric Power Co., LTD. Research Institute. His research interests are direct current distribution network active distribution network and power distribution, and energy saving technology.